Dental Materials Journal 25(2) : 316−331, 2006

Sulfuration Resistance of Five Experimental Ag-Pd-Au-Cu Alloys with Low Pd Content of 10 or 12%

Setsuo SAITOH, Yoshima ARAKI and Masayuki TAIRA
Department of Dental Materials Science and Technology, Iwate Medical University School of Dentistry, 1-3-27, Chuo-dori, Morioka, Iwate 020-8505, Japan
Corresponding author, Setsuo Saitoh E-mail:setsuos@iwate-med.ac.jp

Received June 22, 2005/Accepted March 2, 2006

Commercial Ag-based alloy (46Ag-20Pd-12Au-20Cu alloy) is widely used in Japan as a casting alloy. As opposed to the commercial composition, we prepared five experimental Ag-based alloys with reduced Pd content of 10 or 12%, increased Au content of 20 to 30%, and reduced Cu content of 12 to 20%. We then evaluated their sulfuration resistance by analyzing cast specimen surfaces dipped in 0.1% Na_2S solution with SEM/EPMA, TF-XRD, and XPS. It became evident that all alloys were susceptible to sulfuration in the segregated Ag-rich Pd-poor phases. The degree and speed of sulfuration, however, differed among the six alloys examined. In particular, one experimental alloy (46Ag-10Pd-30Au-12Cu) possessed a sulfuration resistance equal or superior to that of commercial Ag-based alloy, while the other four experimental alloys were inferior in sulfuration resistance. Based on the results of this study, we concluded that our newly developed 46Ag-10Pd-30Au-12Cu alloy could be employed as a new sulfuration-resistant Ag-based casting alloy − which is especially useful if the price of Pd is skyrocketing again.

Key words: Ag-Pd-Au-Cu alloys, Low Pd content, Sulfuration resistance

INTRODUCTION

Ag-Pd-Au-Cu alloys with many different compositions (basically, Ag-based alloys) have been developed in Japan[1−3]. With due consideration to the factors of price, strength, and sulfuration resistance, Ag-20Pd-12Au-Cu alloys with varying contents of Ag (*circa* 46%) and Cu (*circa* 20%) are routinely used as cast inlays, crowns and bridges in Japanese dental clinics[1,2]. However, the major drawback of Ag-based alloys lies in the sulfuration of Ag matrix[4−6]. To circumvent this problem, Pd and Au are usually added[1,2].

Six years ago, due to the very high price of Pd, there was a strong intent to partially replace Pd content with Au content in Ag-20Pd-Au-Cu alloys[7]. To this end, Yoshida *et al.* and Endo *et al.* have developed new Ag-Pd-Au-Cu alloys with Pd contents of 5%[7,8] and 15%[5] respectively − both of which demonstrated adequate strength and sulfuration resistance. To date, no other related systematic studies have since been reported. Although presently, Pd costs lower than Au, there is always a lurking possibility of another price increase because Pd is produced only in politically unstable countries[1,2]. Against this background, it is still important to develop new Ag-Pd-Au-Cu alloys with less Pd content[1,2].

In our new Ag-Pd-Au-Cu alloy system, we designed five alloy compositions based on the strategy to reduce Pd content from the standard control of 20% to a pre-set 10 or 12% while altering Ag (between 38 and 46%), Cu (between 12 and 20%), and Au (between 20 and 30%) contents.

To evaluate the sulfuration resistance of Ag-based alloys, the immersion test in Na_2S solution has often been conducted[9−13]. Sulfurated or corroded surfaces were then analyzed using scanning electron microscopy/electron probe microanalysis (SEM/EPMA)[14,15], X-ray diffraction (XRD)[16,17], and X-ray photoelectron spectroscopy (XPS)[5,18−21].

The aims of this investigation were to: (1) examine metallography by SEM/EDX; and (2) evaluate sulfuration resistance by SEM/EPMA, thin film (TF)-XRD, and XPS of cast one commercial Ag-20Pd-12Au-Cu alloy (control) and five experimental self-prepared Ag-low Pd-(10 to 12%)Au-Cu alloys.

MATERIALS AND METHODS

Alloy design

Table 1 shows the compositions, molar fractions of Pd + Au, and codes of control commercial Ag-20Pd-12Au-Cu alloy and five experimental Ag-low Pd-Au-Cu alloys examined in this study. The sum of molar fraction of Pd and Au increased from 0.218 (EX-1) to 0.276 (EX-5), while that of PALA was 0.244. Upon our request, five experimental Ag-based alloy plates (about 5×10×1 mm) were manufactured by a commercial company (Nihonbashi Tokuriki Co., Tokyo, Japan).

Specimen preparation by casting

Six Ag-based alloy specimens (either 6×6×1.5 mm or 20×20×0.4 mm) were prepared by lost wax cast-

Table 1 Compositions, molar fractions of Pd + Au, and codes of control and five experimental Ag-low Pd-Au-Cu alloys

	Composition (wt%)						Molar fraction of Pd+Au	Code
	Ag	Pd	Au	Cu	Zn	Others		
Control alloy[1]	46	20	12	20	—	2	0.244*	PALA
Experimental alloy 1[2]	46	12	20	20	2	—	0.218	EX-1
Experimental alloy 2[2]	42	12	24	20	2	—	0.242	EX-2
Experimental alloy 3[2]	46	12	24	16	2	—	0.249	EX-3
Experimental alloy 4[2]	38	10	30	20	2	—	0.261	EX-4
Experimental alloy 5[2]	46	10	30	12	2	—	0.276	EX-5

[1]Castwell M.C., GC Co., Tokyo, Japan.
[2]Experimental alloys manufactured by Nihonbashi Tokuriki Co., Tokyo, Japan, upon our request.
*Molar fraction of control alloy was calculated assuming that 'Others' component was zinc.

ing in air with cristobalite investment (conventional type, GC, Tokyo, Japan), blowtorch (Uni-blowpipe, Yoshida, Tokyo, Japan), and centrifugal casting machine (Kerr Centrifico Casting Machine, Kerr, Romulus, USA). All cast specimens were bench-cooled, taken out, abraded in water with #1500 SiC waterproof abrasive papers, followed by fine polishing with 0.3-μm alumina suspension. They were next washed by ultrasonic agitation in acetone and deionized water for 10 minutes each, and then stored in a desiccator for metallography and immersion tests in Na_2S solution.

Metallographic examination of cast specimens

For SEM/EDX, six Ag-based alloy specimens ($6\times6\times1.5$ mm) were dipped in 25% $(NH_4)_2S_2O_8$ solution for 10 minutes, ultrasonically cleaned in deionized water for 10 minutes, and then air-dried naturally. Their metallographic observations and semi-quantitative elemental analyses were conducted using SEM/EDX (S-4700, Hitachi, Tokyo, Japan/EMAX-7000, Horiba Seisakusho, Kyoto, Japan) at an acceleration voltage of 15 kV.

Surface analysis after immersion in 0.1% Na_2S solution

For SEM/EPMA, six Ag-based alloy specimens ($6\times6\times1.5$ mm) were dipped in 15 ml of 0.1% Na_2S solution for one and seven days at 37℃, followed by ultrasonic cleaning in deionized water for 10 minutes and natural air-dry. They were then analyzed with an SEM/EPMA (JXA-8900L, JEOL, Tokyo, Japan). Area scan ($100\times100\,\mu$m) was carried out at an acceleration voltage of 15 kV and a probe current of 6×10^{-8} A to detect the distribution of six elements (S, Ag, Pd, Cu, Zn, and Au) in each alloy.

For TF-XRD, six Ag-based alloy specimens ($20\times20\times0.4$ mm) were dipped in 125 ml of 0.1% Na_2S solution for one and seven days at 37℃, followed by ultrasonic cleaning in deionized water for 10 minutes and natural air-dry. They and un-dippped specimens were then analyzed by TF-XRD with a diffractometer (JDX-3500, JEOL, Tokyo, Japan) using Cu Kα radiation as the X-ray source. Glancing angle of the specimen (θ angle) was fixed at 1° or 3° against the incident beam. Characteristic XRD peaks were then labeled with reference to standard powder diffraction data stored in the diffractometer's workstation.

For XPS, six Ag-based alloy specimens ($6\times6\times1.5$ mm) were dipped in 15 ml of 0.1% Na_2S solution for one day at 37℃, followed by ultrasonic cleaning in deionized water for 10 minutes and natural air-dry. They and un-dipped specimens were then analyzed by XPS in wide and narrow scan modes using an XPS (AXIS-HSi, Kratos, UK) with Mg Kα radiation operated at 15 kV accelerating voltage and 3 mA current under a vacuum of 4×10^{-9} torr. Analysis area on each alloy was an ellipse approximately $200\times600\,\mu$m in diameter. Binding energy scale was calibrated by the C 1s peak at 284.8 eV, while seven elements (S, Ag, Pd, Au, Cu, O, and C) were identified by XPS peaks of S 2p, Ag 3d, Pd 3d, Au 4f, Cu 2p, O 1s, and C 1s respectively.

RESULTS

Metallographic examination of cast specimens

Fig. 1 shows the SEM photomicrographs and (grain) phases revealed by EDX of cast control Ag-20Pd-12Au-Cu alloy and five experimental Ag-low Pd-Au-Cu alloys. All alloys were heterogeneous in composition. Each alloy had two to four different phases with varied elemental compositions among the individual phases.

In terms of phases, PALA had three phases (A, B, and C), EX-1 had four phases (D, E, F, and G), EX-2 had three phases (H, I, and J), EX-3 had three phases (K, L, and M), EX-4 had three phases (N, O, and P), and EX-5 had two phases (Q and R). Nonetheless, each alloy had at least two distinctive phases, namely, Ag-rich Pd-poor phase (C in PALA, G in EX-1, J in EX-2, M in EX-3, P in EX-4, and Q in EX-5) and Ag-poor Pd-rich phase (B in PALA, D and F in EX-1, I in EX-2, L in EX-3, O in EX-4, and R in EX-5).

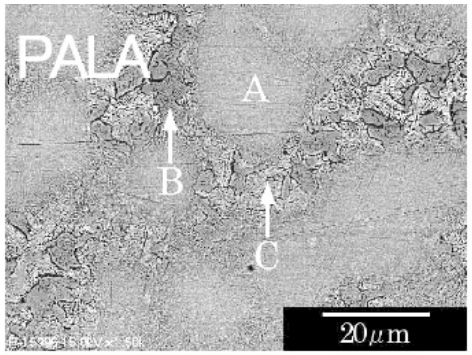

	Ag	Pd	Au	Cu	Zn
A	→	↑	→	→	↑
B	↓	↑	→	↑	↑
C	↑	↓	→	↓	↓

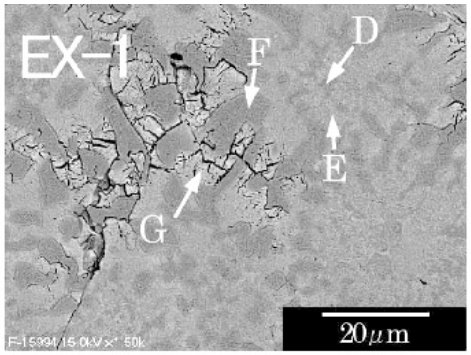

	Ag	Pd	Au	Cu	Zn
D	↓	↑	→	↑	↑
E	→	→	→	↓	→
F	↓	↑	→	↑	↑
G	↑	↓	→	↓	↓

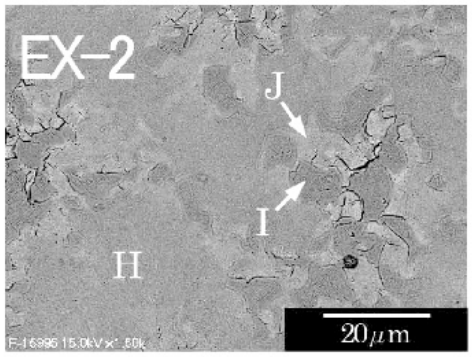

	Ag	Pd	Au	Cu	Zn
H	→	↑	→	→	↑
I	↓	↑	→	↑	↑
J	↑	↓	→	↓	↓

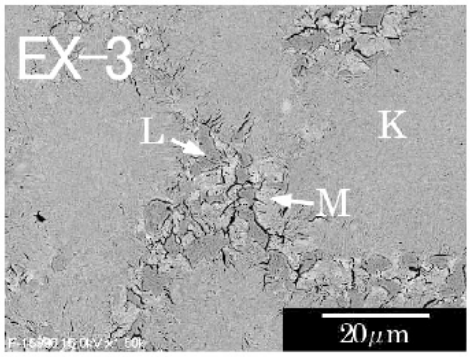

	Ag	Pd	Au	Cu	Zn
K	→↑	→↑	→	→↓	→↑
L	↓	↑	→	↑	↑
M	↑	↓	→	↓	↓

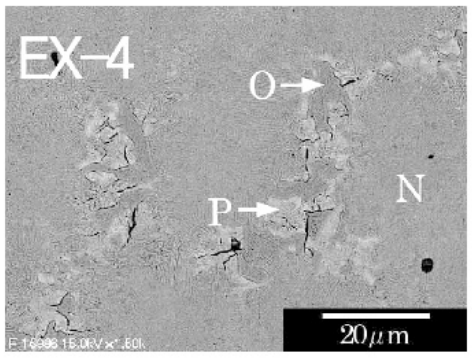

	Ag	Pd	Au	Cu	Zn
N	→	→↑	→	→↓	↑
O	↓	↑	→	↑	↑
P	↑	↓	→	↓	↓

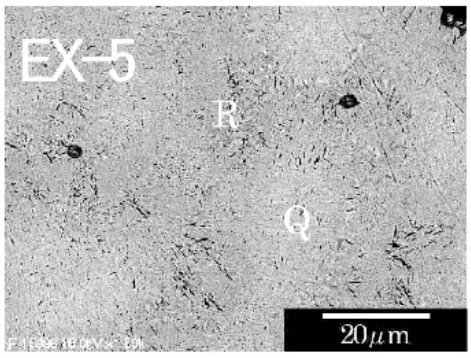

	Ag	Pd	Au	Cu	Zn
Q	↑	↓	→	↓	→
R	↓	↑	→	↑	→

Fig. 1 SEM photographs and phases revealed by EDX of cast control Ag-20Pd-12Au-20Cu alloy and five experimental Ag-low Pd-Au-Cu alloys.

EPMA analyses after immersion in 0.1% Na_2S solution

Figs. 2 to 8 show the black and white EPMA photomicrographs (composition images (CP), element S, element Ag, element Pd, element Cu, element Zn, and element Au) of cast control Ag-20Pd-12Au-Cu alloy and five experimental Ag-low Pd-Au-Cu alloys immersed in 0.1% Na_2S for one day (top) and seven days (bottom), respectively.

On CP in EPMA photomicrographs (Fig. 2), dark and black areas reflect lower atomic weight elements (e.g., S) or voids, while bright and white areas are made up of higher atomic weight elements (e.g., Au). Large black areas formed quickly on EX-1 after one day's immersion and apparently grew after seven days' immersion. Black stains and dots

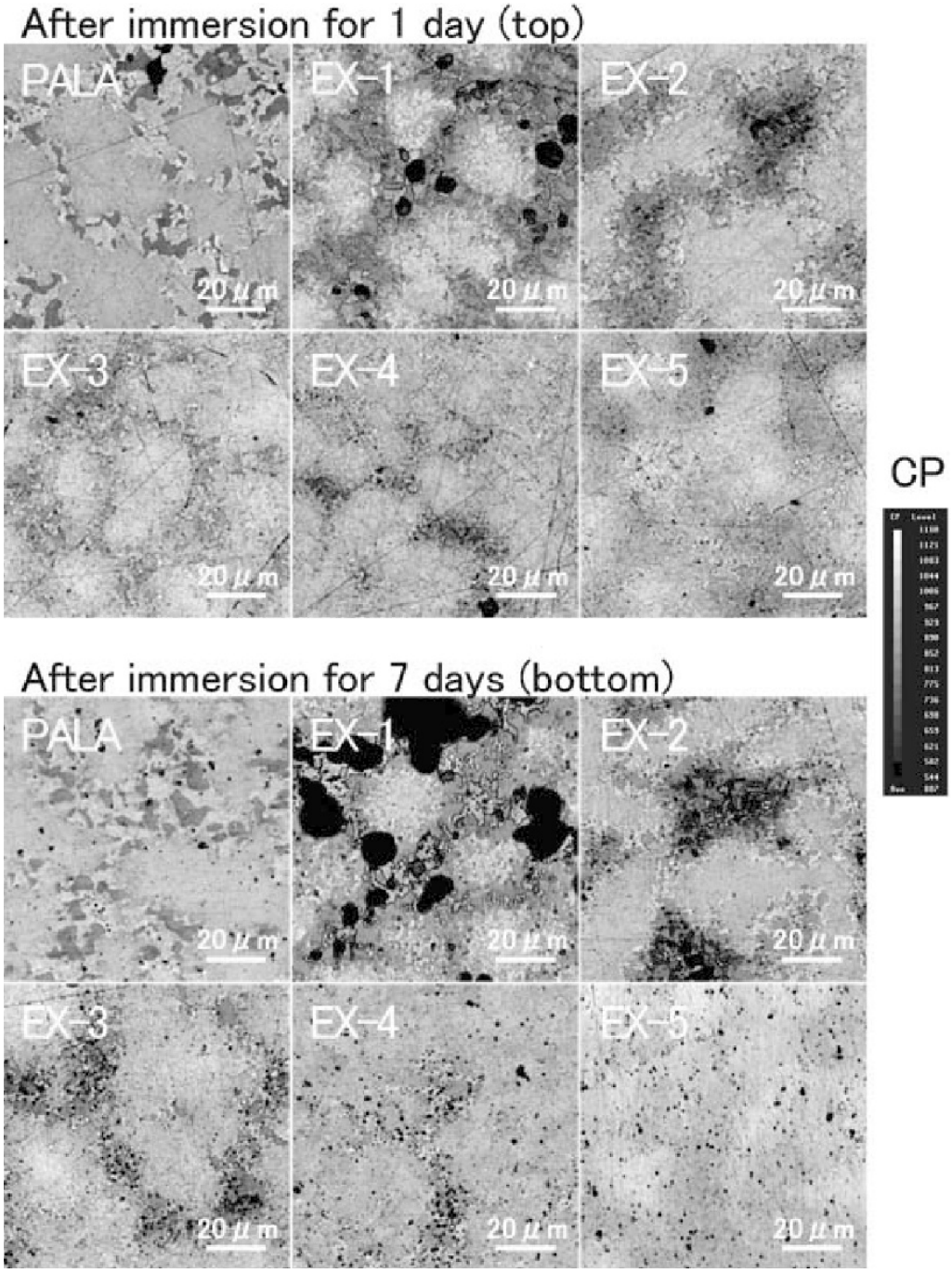

Fig. 2 CP (composition images) in EPMA photomicrographs of cast control Ag-20Pd-12Au-20Cu alloy and five experimental Ag-low Pd-Au-Cu alloys immersed in 0.1% Na_2S for 1 day (top) and 7 days (bottom).

were also observed on the other five alloys, which tended to increase and enlarge as the immersion period increased from one to seven days.

As for black and white EPMA elemental mappings (Figs. 3-8), if a region contains a larger amount of the element searched, it will appear whiter and brighter.

On element S EPMA photomicrographs (Fig. 3), sulfides formed aggressively on EX-1, EX-2, EX-3, and EX-4 after one day's immersion and grew significantly as the immersion period increased to seven days. Little sulfide was produced on PALA and EX-5 after one day's immersion, but precipitated slightly and sparsely after seven days' immersion.

On element Ag EPMA photomicrographs (Fig. 4), considerable segregation of Ag was noticed for

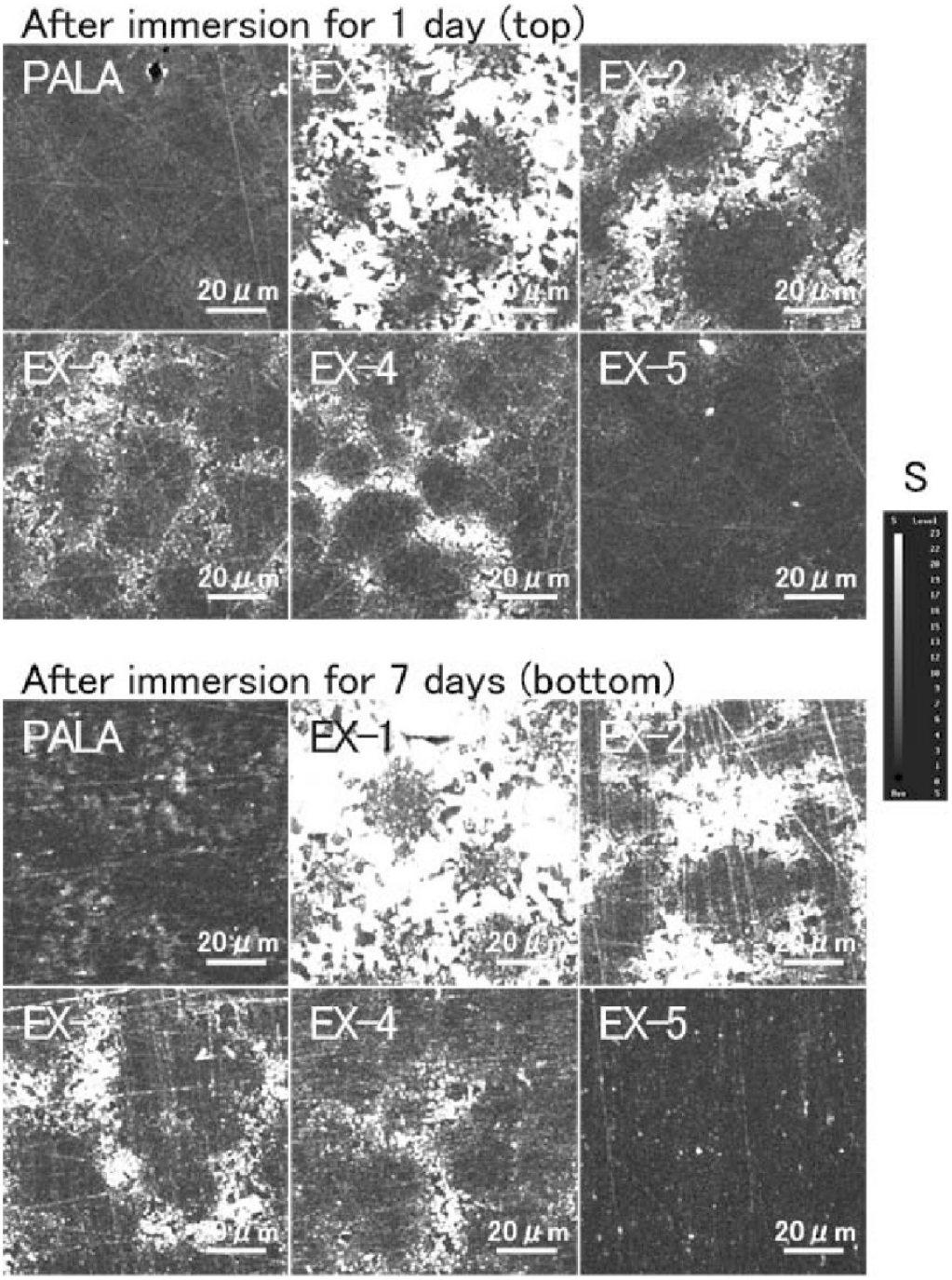

Fig. 3 Element S EPMA photomicrographs of cast control Ag-20Pd-12Au-20Cu alloy and five experimental Ag-low Pd-Au-Cu alloys immersed in 0.1% Na_2S for 1 day (top) and 7 days (bottom).

PALA, EX-1, EX-2, EX-3, and EX-4, but much less for EX-5. Ag-rich areas (Fig. 4) tended to correspond to S-rich areas (Fig. 3).

On element Pd EPMA photomicrographs (Fig. 5), large-scale segregation of Pd was found for PALA, EX-1, EX-2, EX-3, and EX-4, but less for EX-5. Pd-rich areas (Fig. 5) tended to coincide with Ag-poor areas (Fig. 4) and S-poor areas (Fig. 3).

On element Cu EPMA photomicrographs (Fig. 6), large-scale segregation of Cu was likewise seen for PALA, EX-1, EX-2, EX-3, and EX-4, but less for EX-5. Cu-rich areas (Fig. 6) tended to coincide with Pd-rich areas (Fig. 5).

On element Zn EPMA photomicrographs (Fig. 7), large-scale segregation of Zn was confirmed for EX-1, EX-2, EX-3, and EX-4, but small-scale for PALA

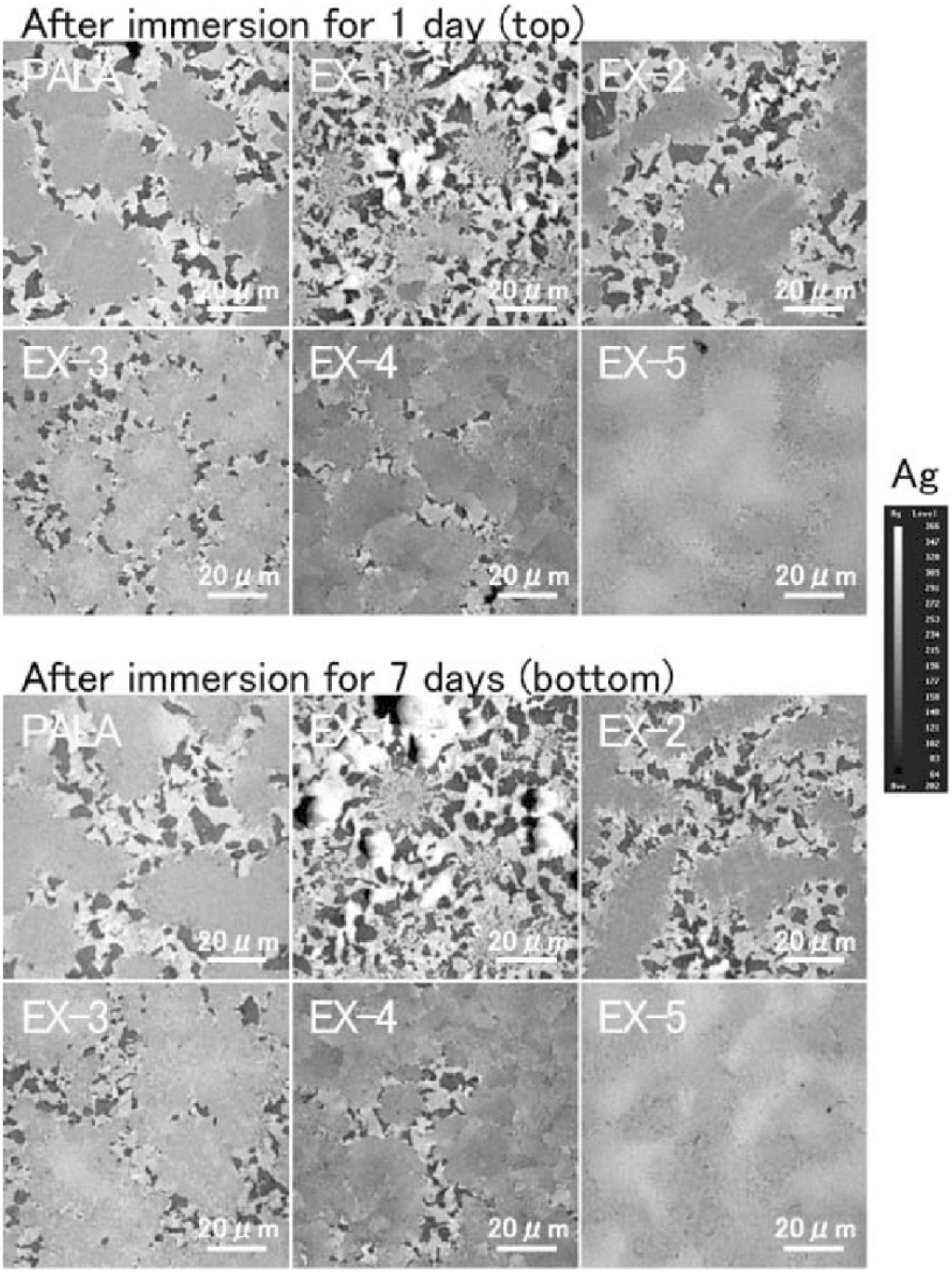

Fig. 4 Element Ag EPMA photomicrographs of cast control Ag-20Pd-12Au-20Cu alloy and five experimental Ag-low Pd-Au-Cu alloys immersed in 0.1% Na_2S for 1 day (top) and 7 days (bottom).

and EX-5. The Zn distributions resembled those of Pd.

On element Au EPMA photomicrographs (Fig. 8), only a slight segregation of Au was found for EX-1. In other words, Au seemed to distribute homogeneously for the other alloys. Black regions on EX-1 (Figs. 5-8) superimposed on S-rich areas (Fig. 3).

Fig. 9 shows the CP and EPMA color photomicrographs of elements S, Ag, Pd, Cu, Zn, and Au of cast one experimental Ag-low Pd-Au-Cu alloy (EX-1) after immersion in 0.1% Na_2S for seven days. With color EPMA, red color depicts presence of high concentration of an element, whilst low concentration and absence of an element are represented by blue and black colors. It was re-confirmed that

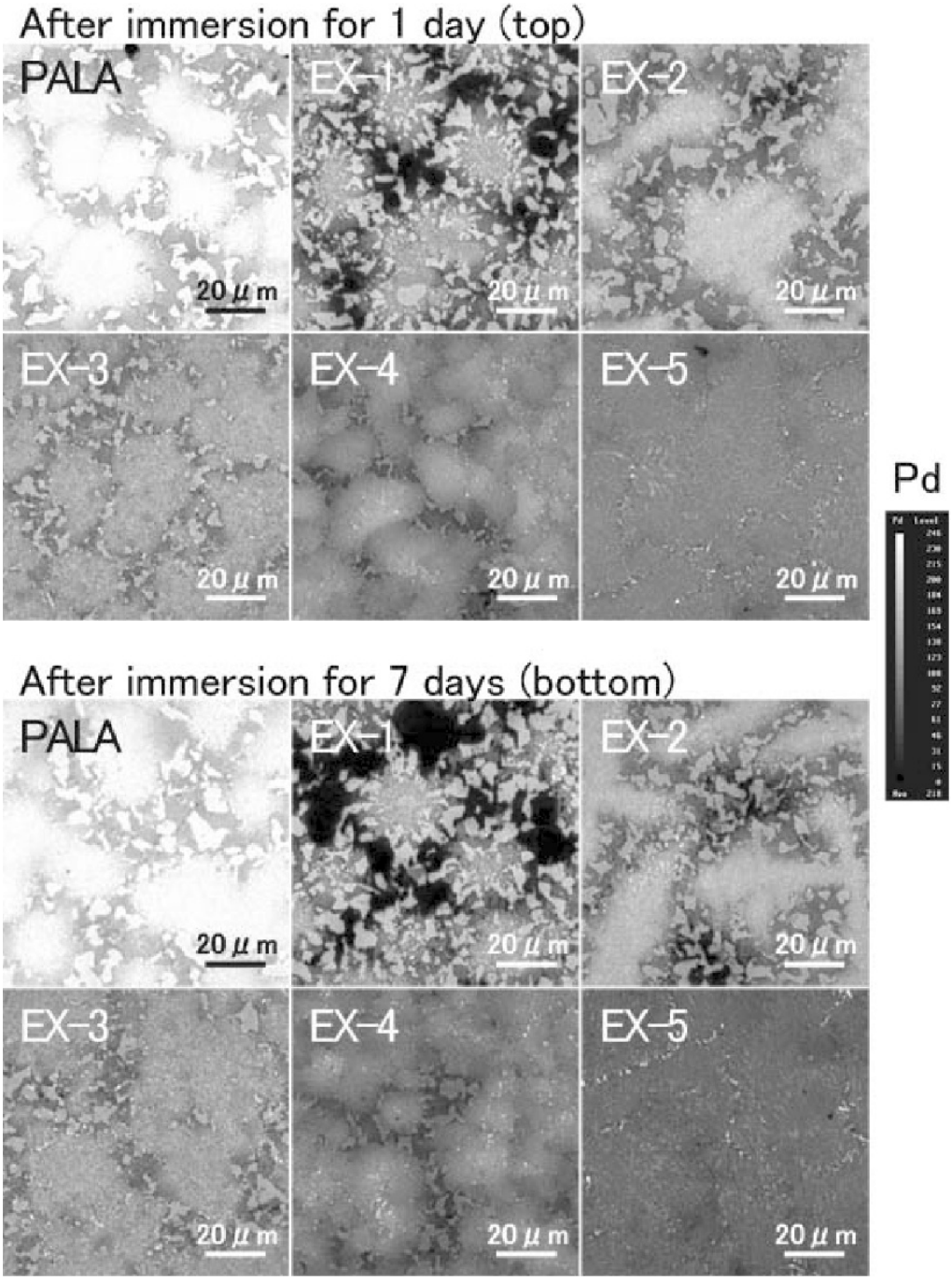

Fig. 5 Element Pd EPMA photomicrographs of cast control Ag-20Pd-12Au-20Cu alloy and five experimental Ag-low Pd-Au-Cu alloys immersed in 0.1% Na_2S for 1 day (top) and 7 days (bottom).

sulfuration preferentially occurred on Ag-rich Pd-poor (virtually Pd-deficient) areas, which appeared black on CP (BSE image). Pd-rich Ag-poor zones, which appeared white on CP, had little coupling with sulfur. The distributions of Cu and Zn were similar to that of Pd, whereas Au appeared to distribute uniformly except the regions where sulfide precipitated.

TF-XRD analyses before and after immersion in 0.1% Na_2S solution

Figs. 10(a) to 10(c) show the TF-XRD patterns of control Ag-20Pd-12Au-20Cu alloy and five experimental Ag-low Pd-Au-Cu alloys before immersion in 0.1% Na_2S, after immersion in Na_2S for one day, and after immersion in Na_2S for seven days respectively. Fig. 10(d) then shows the peak labeling of the crys-

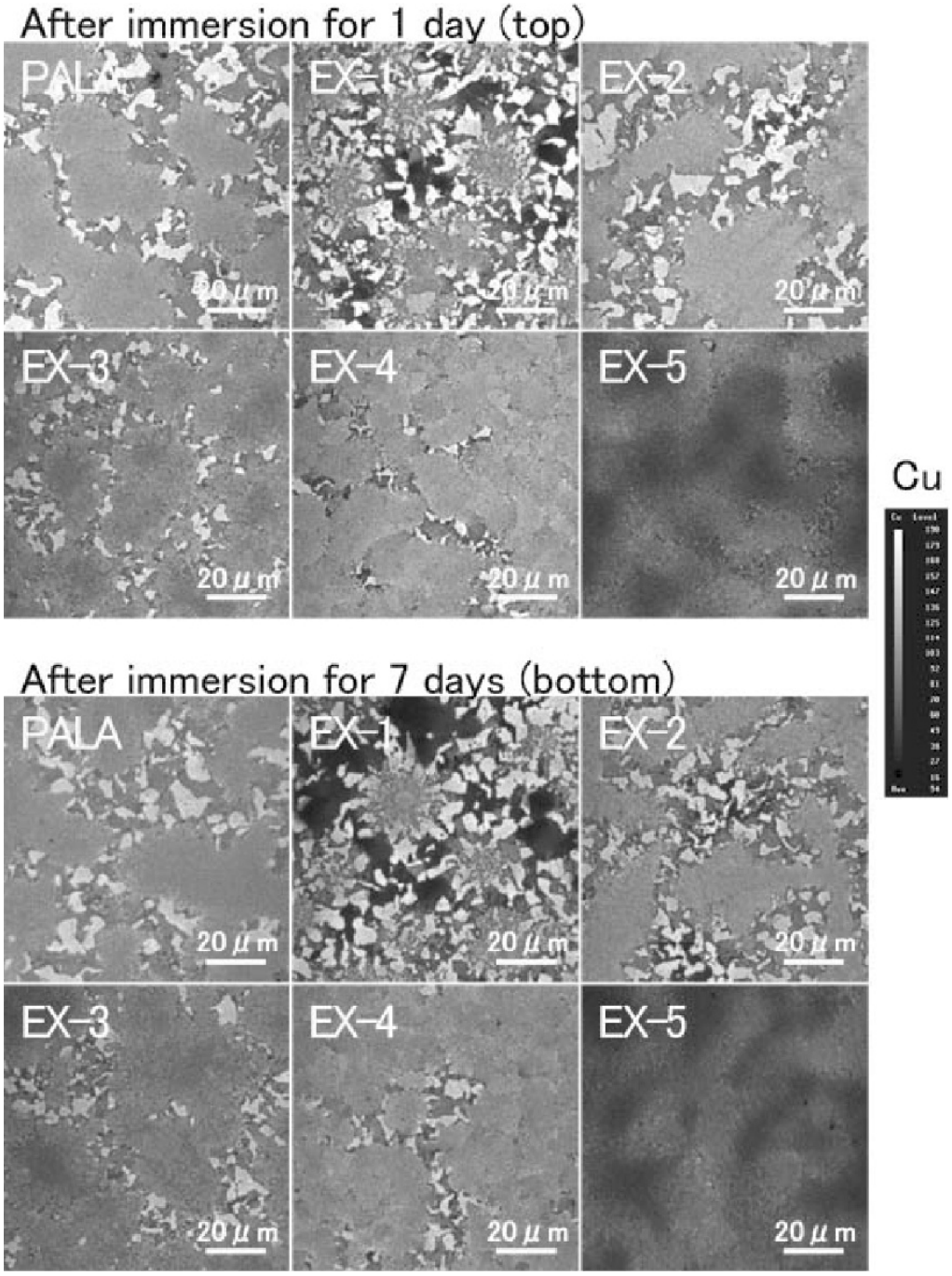

Fig. 6 Element Cu EPMA photomicrographs of cast control Ag-20Pd-12Au-20Cu alloy and five experimental Ag-low Pd-Au-Cu alloys immersed in 0.1% Na_2S for 1 day (top) and 7 days (bottom).

tals formed on one experimental Ag-low Pd-Au-Cu alloy (EX-1) which was dipped in Na_2S for seven days.

Before immersion, all the six alloys studied possessed five similar peaks and shoulders in the 2θ angle region between 38° and 48°, indicating that all the alloys were basically made up of similar Ag-based metallic phases (Fig. 10(a)).

Immersion in Na_2S for one day did not produce any detectable S-related XRD peaks on all the six alloys' surfaces (Fig. 10(b)). As a result, the peaks were analogous to those before immersion (Fig. 10(a)).

On the other hand, immersion in Na_2S for seven days caused noticeable S-related peaks (16 dotted lines) in addition to the five original alloy (M) peaks

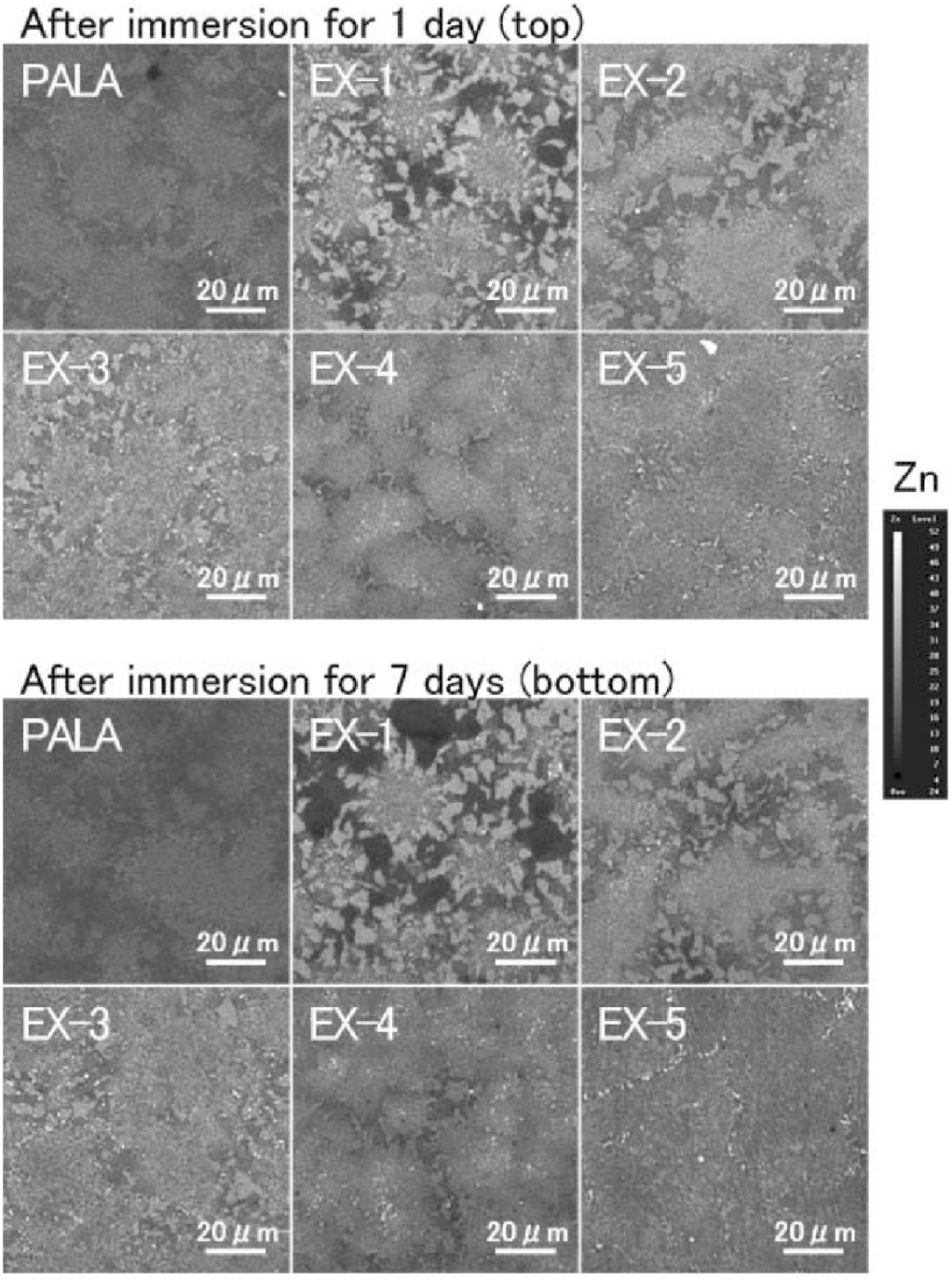

Fig. 7 Element Zn EPMA photomicrographs of cast control Ag-20Pd-12Au-20Cu alloy and five experimental Ag-low Pd-Au-Cu alloys immersed in 0.1% Na_2S for 1 day (top) and 7 days (bottom).

(five solid lines) (Fig. 10(c)). These new peaks appeared on identical 2θ angles for all the six alloys examined, but the peak heights differed among the six alloys. EX-1 had the strongest intensity for the new peaks, followed by EX-2, PALA, EX-3, and EX-4 in this order, whilst EX-5 had the weakest intensity.

On EX-1 which was immersed in Na_2S for seven days, a detailed XRD peak labeling was performed (Fig. 10(d)). Besides five original metal (M) peaks, 16 characteristic peaks were identified as those of three metal sulfides — Ag_2S, Cu_2S, and PdS. The peaks of Ag_2S were predominant while those of Cu_2S and PdS were very small, suggesting that Ag_2S was a dominant metal sulfide which precipitated on all the six Ag-based alloys after immersion in Na_2S for seven days.

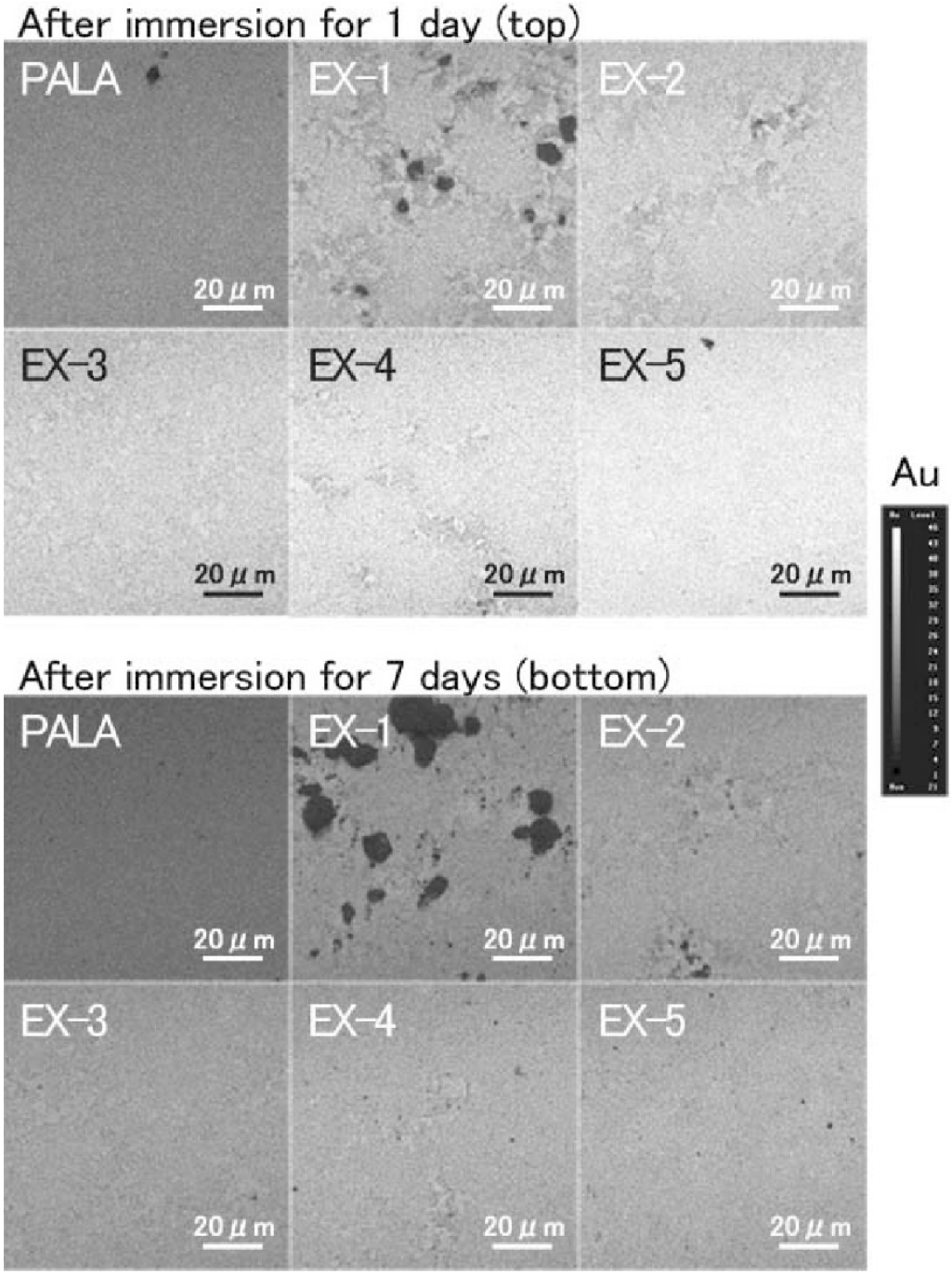

Fig. 8 Element Au EPMA photomicrographs of cast control Ag-20Pd-12Au-20Cu alloy and five experimental Ag-low Pd-Au-Cu alloys immersed in 0.1% Na_2S for 1 day (top) and 7 days (bottom).

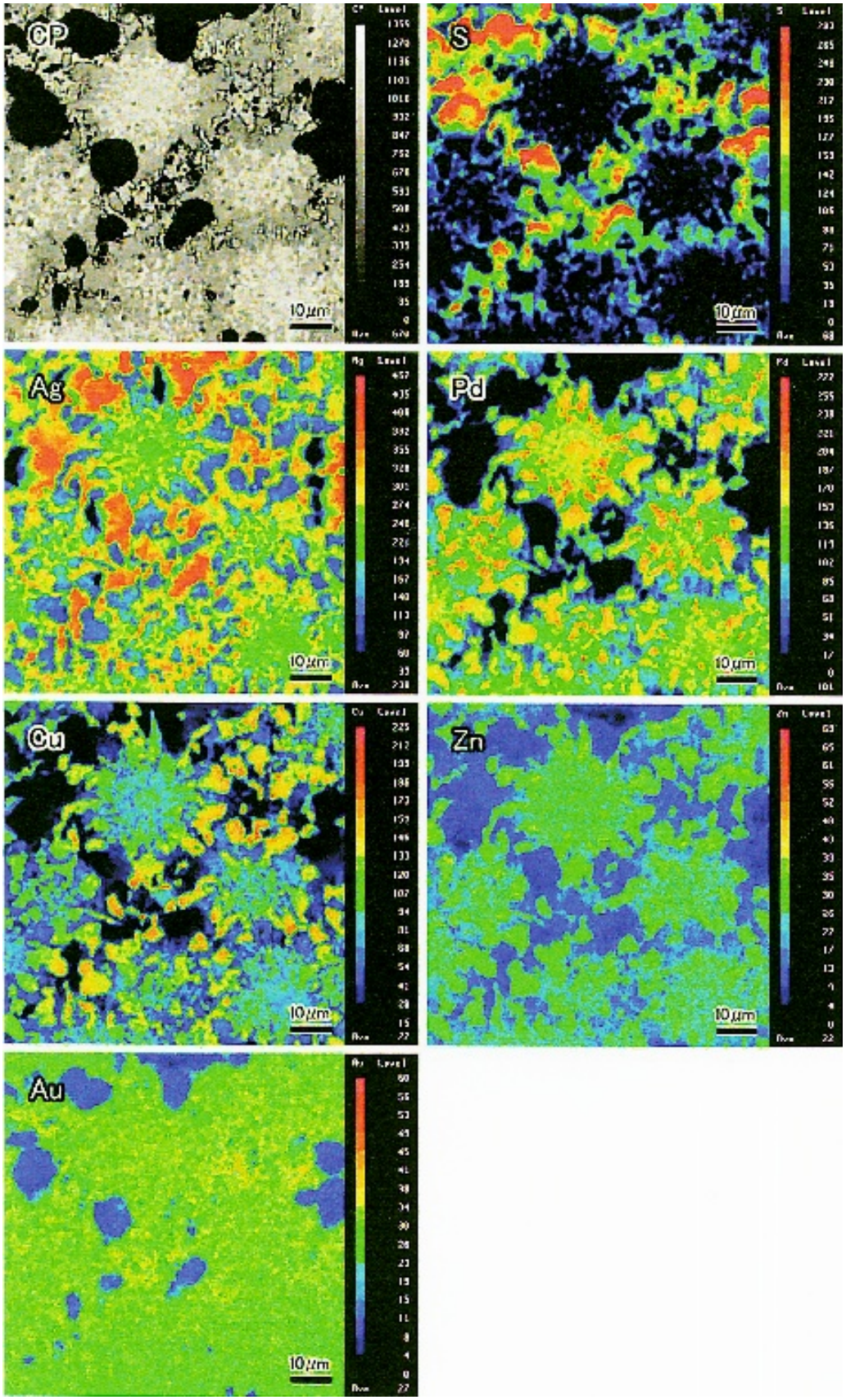

Fig. 9 CP (composition image) and EPMA color photomicrographs of elements S, Ag, Pd, Cu, Zn, and Au of cast one experimental Ag-low Pd-Au-Cu alloy (EX-1) after immersion in 0.1% Na_2S for 7 days.

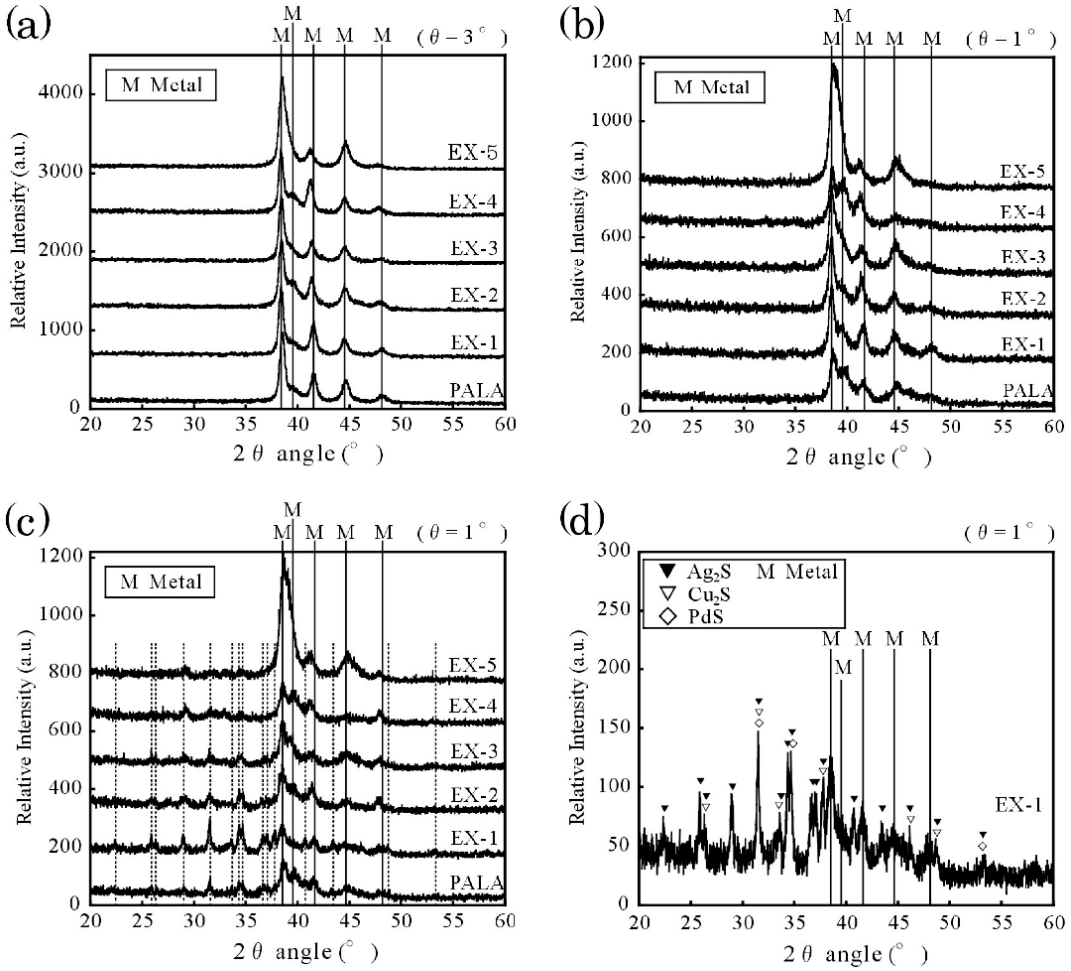

Fig. 10 TF-XRD patterns of cast control Ag-20Pd-12Au-20Cu alloy and five experimental Ag-low Pd-Au-Cu alloys: (a) before immersion in 0.1% Na_2S; (b) after immersion in 0.1% Na_2S for 1 day; (c) after immersion in 0.1% Na_2S for 7 days; and (d) peak labeling of the crystals formed on EX-1 which was dipped in 0.1% Na_2S for 7 days.

XPS analyses after immersion in 0.1% Na_2S solution

Fig. 11 shows the XPS wide scan spectra of the uppermost layer of cast control Ag-20Pd-12Au-20Cu alloy and five experimental Ag-low Pd-Au-Cu alloys after immersion in 0.1% Na_2S for one day. It became clear that S peaks (S 2p and S 2s) (labeled by two big arrows) were superimposed onto the peaks of original cast and polished alloy surfaces, such as those of Cu 2p, Ag 3d, Pd 3d, and Au 4f, *etc.*, suggesting that sulfuration — which was detected by XPS — actually occurred on all the alloys after immersion in 0.1% Na_2S for only one day. Besides Cu, Ag, Pd, and Au elements, O KLL was also found present as oxides and C 1s as contaminated hydrocarbon.

Fig. 12 shows the XPS narrow scan spectra of the uppermost layer of cast control Ag-20Pd-12Au-20Cu alloy and five experimental Ag-low Pd-Au-Cu alloys after immersion in 0.1% Na_2S for one day. There were no remarkable differences in characteristic spectra shapes among the six Ag-based alloys,

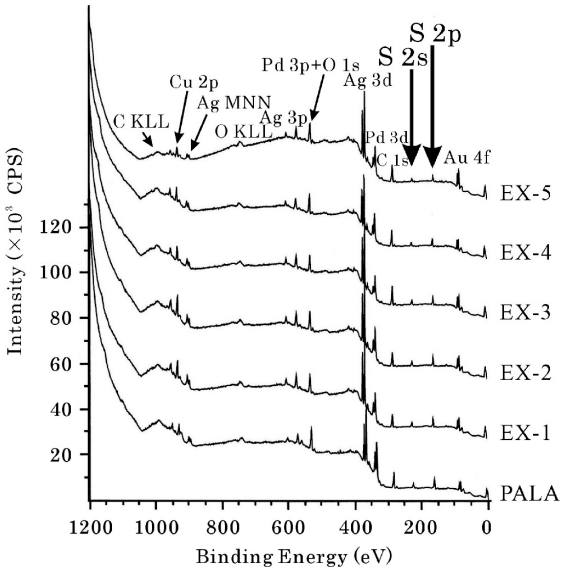

Fig. 11 XPS wide scan spectra of the uppermost layer of cast control Ag-20Pd-12Au-20Cu alloy and five experimental Ag-low Pd-Au-Cu alloys after immersion in 0.1% Na_2S for 1 day.

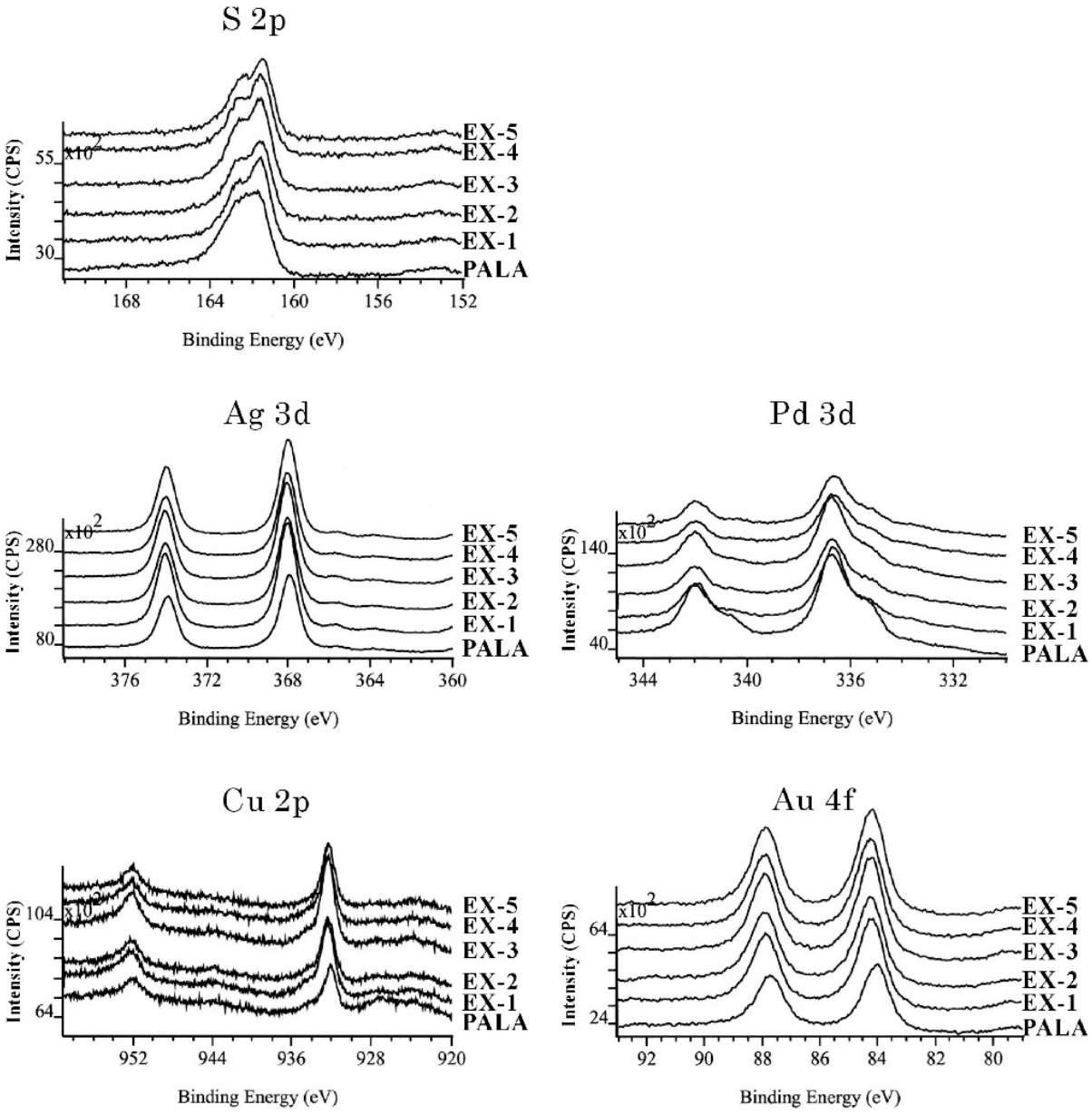

Fig. 12 XPS narrow scan spectra of the uppermost layer of cast control Ag-20Pd-12Au-20Cu alloy and five experimental Ag-low Pd-Au-Cu alloys after immersion in 0.1% Na_2S for 1 day, whereby the spectra corresponded to the five elements of S, Ag, Pd, Cu, and Au.

whereby the spectra corresponded to the five elements of S, Ag, Pd, Cu, and Au. This finding implied that sulfides formed on all the six alloy surfaces − after dipping in 0.1% Na_2S solution for only one day − were basically identical.

DISCUSSION

By SEM/EDX, we observed significant phase segregation[22,23] in five alloys (PALA, EX-1, EX-2, EX-3, and EX-4) out of six alloys after casting (Fig. 1). The reason for this segregation phenomenon is unclear, but alloy melting and slow cooling during casting might produce such segregations[23]. Phase segregations are undesirable for sulfuration resistance, because sulfuration-vulnerable Ag-rich Pd-poor phases are produced[5]. One alloy (EX-5) was least phase-segregated, and had two phases consisting of relatively analogous chemical compositions of Ag, Pd, Cu, Zn, and Au (Fig. 1), which seemed to be advantageous in terms of sulfuration resistance.

We employed three different techniques to evaluate the sulfuration of Ag-based alloys. Approximate detection depths of SEM/EPMA, TF-XRD, and XPS

were 100 nm, 500 nm, and 5 nm respectively. Therefore, with SEM/EPMA and XPS, we could trace the sulfides formed on the examined alloys after immersion in 0.1% Na_2S for one short day, but not so with TF-XRD. After immersion for seven days, the enlarged sulfides could be identified by both SEM/EPMA and TF-XRD. In the evaluation of the sulfuration resistance of six Ag-based alloys, alloy surfaces immersed in 0.1% Na_2S for one and seven days were regarded as standard and accelerated conditions respectively.

It was judged from SEM/EPMA (Figs. 2-9) and TF-XRD (Fig. 10) analyses that all Ag-based alloys were sulfurated in Ag-rich Pd-poor areas. Degree of sulfuration and reaction kinetics, however, varied depending on the alloy type. The six Ag-based alloys examined could be classified into two groups: Group 1 — fast and intensely sulfurated group — to which EX-1, EX-2, EX-3, and EX-4 belonged; Group 2 — slow and slightly sulfurated group — to which PALA and EX-5 belonged. The sulfides identified were mostly Ag_2S, while PdS and Cu_2S were found in smaller quantities (Fig. 10(d)). Considering that Cu and Zn distributions were similar to that of Pd, and that Au distributed homogeneously, the growing sulfuration of all the six Ag-based alloys examined might occur predominantly between Ag and S in Ag-rich Pd-poor, Cu-poor, and Zn-poor phases. However, it should be noted that for all the six Ag-based alloys dipped in 0.1% Na_2S for only one day, their XPS peak heights of S 2p were similar (Figs. 11 and 12). This finding might serve to support the hypothesis that upon exposure to 0.1% Na_2S solution, the entire uppermost surface of Ag-based alloys was instantaneously covered by an ultra-thin sulfur tarnish layer (around 10 nm) presumably made up of Ag_2S and PdS[5]. If the alloy is not resistant to further sulfuration, silver sulfide (Ag_2S) might grow rapidly and predominantly in Ag-rich Pd-poor phases to the extent whereby TF-XRD can detect with a large diffraction peak[5]. On the contrary, if the alloy is resistant to further sulfuration, the sulfide layer might grow very slowly such that only a weak intensity for Ag_2S peak was registered.

In addition to analyses by SEM/EPMA, TF-XRD, and XPS, an attempt is made here to compare the sulfuration resistance of the six Ag-based alloys based on their compositions (Table 1). There is a general understanding that Pd and Au strongly and moderately retard the sulfuration of Ag[24,25], respectively. On the other hand, Cu moderately accelerates sulfuration[26]. Based on these notions, EX-1 (8% less Pd and 8% more Au than PALA) was most susceptible to sulfuration, implying that a mere simple substitution of Pd with Au could not maintain the sulfuration resistance of control PALA. Likewise, EX-2, EX-3, and EX-4 — which had 0 to 8% less Ag, 8 to 10% less Pd, 12 to 18% more Au, and 0 to 4% less Cu than PALA — could not maintain the sulfuration resistance of control PALA. Only EX-5 — which had 10% less Pd, 18% more Au, and 8% less Cu than PALA — possessed a sulfuration resistance equal or superior to that of control PALA. We believed that the excellent sulfuration resistance of EX-5 could be attributed to two factors: (i) increase of Au by 18% and decrease of Cu by 8%, while reducing Pd content by 10%; and (ii) phase segregation of a smaller scale as mentioned above.

At this juncture, we have completed the evaluation of the sulfuration resistance of five experimental Ag-(10 to 12%)Pd-Au-Cu alloys. However, it also seems to be necessary to carry out further studies that entail castability tests[27,28], mechanical strength tests[29,30], and biocompatibility tests[31—33] in order to thoroughly clarify the practical usefulness of our newly developed EX-5 (46Ag-10Pd-30Au-12Cu alloy). If confirmed to be a viable substitute for PALA, EX-5 would be a useful casting alloy in future dental clinics when the Pd price surges again.

CONCLUSIONS

In the present study, five experimental Ag-low Pd(10 to 12%)-Au-Cu alloys were prepared in a bid to substitute a commercial Ag-based alloy (46Ag-20Pd-12Au-20Cu alloy) (control). To this end, cast specimens were made, metallography was examined, and their sulfuration resistance was evaluated by SEM/EPMA, TF-XRD, and XFS after immersion in 0.1% Na_2S solution. All alloys were phase-segregated, and sulfuration occurred predominantly in Ag-rich Pd-poor phases with different degrees, depending on the alloy type. In particular, one experimental alloy (46Ag-10Pd-30Au-12Cu alloy) possessed a sulfuration resistance equal or superior to that of the commercial Ag-based alloy, which could be due to the following factors:

(i) In terms of composition, the experimental Ag-low Pd-Au-Cu alloy had a Pd content 10% less than that of the commercial 46Ag-20Pd-12Au-20Cu alloy. However, its content of Au — a moderate sulfuration retarder — was 18% more than the control alloy, while its content of Cu — a moderate sulfuration accelerator — was 8% less than the control alloy. Taken together, this composition enabled the experimental alloy to possess excellent sulfuration resistance;

(ii) In terms of phase segregation, it was a small-scale one for the experimental alloy as the compositions of Ag-rich Pd-poor phase and Ag-poor Pd-rich phase were relatively analogous. Further, the Ag-rich Pd-poor phase was still sulfuration-resistant.

If proven to be a viable alternative to the commercial 46Ag-20Pd-12Au-20Cu alloy, this newly developed 46Ag-10Pd-30Au-12Cu alloy is a potential cast-

ing alloy candidate in future dental clinics when the price of Pd surges again.

ACKNOWLEDGEMENTS

This research was supported in part by a Grant-in-aid for High-Tech Research Project (2005-2009), as well as by Grants-in-aid for Scientific Research (Nos. 14571858 and 17592037) from the Ministry of Education, Culture, Sports, Science and Technology, Japan.

REFERENCES

1) The Committee on Evaluation and Status Reports of Dental Materials and Devices. A review and the future in dental casting Au-Ag-Pd alloys. Part 1: Literature survey and alternatives to dental Au-Ag-Pd alloys. J J Dent Mater 2003; 22: 531-563.
2) The Committee on Evaluation and Status Reports of Dental Materials and Devices. A review and the future in dental casting Au-Ag-Pd alloys. Part 2: The basic properties database of Au-Ag-Pd-Cu alloys. J J Dent Mater 2003; 22: 564-598.
3) Okazaki K. Studies on Au-Ag-Pd-Cu alloys. Part 1: Effects of Au component on some properties of alloys. J Japan Soc Dent Appar Mat 1979; 20: 233-239.
4) Niemi L, Holland RI. Tarnish and corrosion of a commercial dental Ag-Pd-Cu-Au casting alloy. J Dent Res 1984; 63: 1014-1018.
5) Endo K, Ohno H. Microstructure and anodic polarization behavior of experimental Ag-18Cu-15Pd-12Au alloy in aqueous sulfide solution. J Mater Sci 2003; 14: 427-434.
6) Endo K, Araki Y, Kawashima I, Yamane Y, Ohno H, Matsuda K. *In vitro* study on the corrosion behavior of three commercial Ag-Pd-Cu-Au alloys in Ringer's and 0.1% Na_2S solutions. Higashi Nippon Shigaku Zassi 1989; 8: 155-163.
7) Yoshida T, Miyasaka T, Okamura H, Oka K, Yamazaki E, Naruse S, Asaki T, Doi Y. Properties of low karat gold alloys. Part 1: Mechanical properties of the alloys containing 5 mass% Pd. J J Dent Mater 2002; 21: 285-293.
8) Matsumoto M, Hattori M, Hasegawa K, Yoshinari M, Kawada E, Oda Y, Mamada K, Yoshida T. Property of low karat gold alloys. Part 2: Corrosion resistance and tarnish of the alloys containing 5 mass% Pd. J J Dent Mater 2002; 21: 302-307.
9) Lang BR, Bernier SH, Giday Z, Asgar K. Tarnish and corrosion of noble metal alloys. J Prosthet Dent 1982; 48: 245-252.
10) Tsuruta S. Tarnish and corrosion of silver alloys in Na_2S solution. Aichi-Gakuin Dent Sci 1993; 31: 243-259.
11) Mueller HJ, Lenke JW, Bopna MS. Surface analysis of tarnished dental alloys. Scanning Microsc 1988; 2: 777-787.
12) Yamatoya F, Nakamura K, Goto S. Effects of gold addition for the properties of casting Pd-Cu-Ag alloy. J J Dent Mater 1985; 4: 730-753.
13) Koyama K. Tarnish/corrosion and microstructure of silver-base and copper-base casting alloys. Aichi-Gakuin Dent Sci 1996; 34: 481-498.
14) Takada Y, Okuno O. Effect of heat history on the corrosion of ferritic stainless steels used for dental magnetic attachments. Dent Mater J 2005; 24: 391-397.
15) Tuccillo JJ, Nielsen JP. Microprobe analysis of an *in vivo* discoloration. J Prosthet Dent 1974; 31: 285-289.
16) Ochi M, Endo K, Ohno H, Takasusuki N, Matsubara H, Maida T. *In vitro* corrosion of dental Ag-based alloys in polyvinylpyrrolidone iodine solution. Dent Mater J 2005; 24: 422-427.
17) Niemi L, Hero H. The structure of a commercial dental Ag-Pd-Cu-Au casting alloy. J Dent Res 1984; 63: 149-154.
18) Endo K, Ohno H, Matsuda K, Asakura S. Electrochemical and surface studies on the passivity of a dental Pd-based casting alloy in alkaline sulphide solution. Corros Sci 2003; 45: 1491-1504.
19) Suoninen E, Hero H. Effect of palladium on sulfide tarnishing of noble metal alloys. J Biomed Mater Res 1985; 19: 917-934.
20) Wataha JC, Malcolm CT. Effect of alloy surface composition on release of elements from dental casting alloys. J Oral Rehabil 1996; 23: 583-589.
21) Niemi L, Minni E, Ivaska A. An electrochemical and multispectroscopic study of corrosion of Ag-Pd-Cu-Au alloys. J Dent Res 1986; 65: 888-891.
22) Chen KI, Lin JH, Ju CP. Microstructure and segregation behavior of palladium in silver-copper-palladium alloys. J Dent Res 1996; 75: 1497-1502.
23) Drapal S, Pomajbik J. Segregation in precious-metal dental-casting alloys. J Dent Res 1993; 76: 587-591.
24) Vaidyanathan TK, Prasad A. *In vitro* corrosion and tarnish analysis of the Ag-Pd binary system. J Dent Res 1981; 60: 707-715.
25) Nakamura T, Nakamura K, Goto S. Effects of gold addition on the properties of casting 20 Pd-5～20 Cu-Ag alloys. J J Dent Mater 1995; 14: 69-86.
26) Kifune T, Nakamura K, Goto S. Properties of the casting Ag-Pd-Cu alloys. J J Dent Mater 1987; 6: 768-787.
27) Watanabe I, Woldu M, Watanabe K, Okabe T. Effects of casting method on castability of titanium and dental alloys. J Mater Sci Mater Med 2000; 11: 547-553.
28) Wang TJ, Kobayashi E, Doi H, Yoneyama T. Castability of Ti-6Al-7Nb alloy for dental casting. J Med Dent Sci 1999; 46: 13-19.
29) Churnjitapilom P, Goto S, Ogura H. Effects of heat treatments and Sn, Ga and In additives on mechanical properties of 35Ag-30Pd-20Au-15Cu alloy. Dent Mater J 2004; 23: 474-489.
30) Goto S, Nakai A, Miyagawa Y, Ogura H. Development of Ag-Pd-Au-Cu alloys for multiple dental applications. Part 2: Mechanical properties of experimental Ag-Pd-Au-Cu alloys containing Sn or Ga for ceramic-metal restorations. Dent Mater J 2001; 21: 135-147.
31) Taira M, Sasaki M, Yamaura-Tanaka C, Saitoh S, Kimura S, Araki Y. Effects of Ni^{2+} ions on cell viability and NO production of murine peritoneal exudates cells (macrophages) with and without lipopolysaccharide stimulation. Dent Mater J 2005; 24:

304-310.
32) Niemi L, Hensten-Pettersen A. *In vitro* cytotoxicity of Ag-Pd-Cu-based casting alloys. J Biomed Mater Res 1985; 19: 549-561.
33) Niemi L, Syrjanen S, Hensten-Pettersen A. The biocompatibility of a dental Ag-Pd-Cu-Au-based casting alloy and its structural components. J Biomed Mater Res 1985; 19: 535-548.